Shack-Hartmann Type Laser Wavefront Sensor for Measuring Electron Density in Low Current Arc

Yuki Inada [a], Shigeyasu Matsuoka [a], Akiko Kumada[a], Hisatoshi Ikeda[a] and Kunihiko Hidaka[a]

[a] Department of Electrical Engineering and Information Systems, Tokyo University, 3-1, Hongo, 7-chome, Bunkyo-ku, Tokyo, Japan

inada@hvg.t.u-tokyo.ac.jp

***Abstract* — A Shack-Hartmann type laser wavefront senor was developed for achieving electron density distributions over an arc channel in an extinguishing phase by only a single measurement with high temporal and spatial resolutions. The sensor was applied to pulsed arcs in 3-mm air gap between rod-to-rod tungsten electrodes with a diameter of 1mm. Electron densities in the arc discharges with currents of several tens of amperes were lower around the gap centre than near the anode and cathode. The behaviour of the electron densities was consistent with the intensity of emission light from arc discharges.**

***Keywords* — Shack-Hartmann, arc discharge, electron density**

I. INTRODUCTION

A fundamental understanding of the behaviour of arc discharges under high pressure is important for the development of highly reliable SF_6 gas circuit breakers, stable arc welding processes and effective decomposition of toxic waste [1-3]. In general, the characteristics of discharges are described by several physical quantities. Particle densities in atmospheric arcs, for example, have been extensively measured by various optical techniques [4-6]. Further, numerical simulation of arc modeling has been a powerful tool for studying transient particle compositions and electrical parameters in arc discharges [7, 8]. However, there has never been a particle density distribution over an arc channel obtained by only a single measurement.

Recently, a Shack-Hartmann type laser wavefront sensor has been demonstrated to be a novel means of achieving number densities of electrons, which play a key role in discharges [9, 10]. We have shown that Shack-Hartmann sensor has great potential as a method for determining an overall electron density distribution at one time with considerable accuracy [11].

In this paper, we report on electron density distributions over atmospheric arc channels in an extinguishing phase with low currents of several amperes. The experimental results obtained by a single measurement using Shack-Hartmann sensor demonstrate the feasibility of fully understanding the unstable extinguishing process of atmospheric arcs.

II. GENERAL INSTRUCTIONS

A. Shack-Hartmann type laser wavefront sensor

Figure 1 illustrates the main components of the Shack-Hartmann type laser wavefront sensor in this study. The sensor employed commercially available two microlens arrays (SUSS Micro Tec 11-1511-100-000; diameter of microlens=150μm; focal length=38.4mm), two continuous-wave diode lasers (TOPTICA Photonics AG iBEAM-SMART-785-S; wavelength=784nm, Melles Griot 56ICS325; wavelength=408nm) and two ICCD (Intensified Charge-Coupled Devise) cameras (Andor Co., Ltd DH734-18F-73; minimum shutter speed=5ns; pixel size=13μm×13μm; pixel number=1024×1024, Andor Co., Ltd DH734-18U-03; minimum shutter speed=2ns; pixel size=13μm×13μm; pixel number=1024×1024). A detailed description of the optical setup and characteristics of a Shack-Hartmann type laser wavefront senor was published elsewhere [9-12].

The temporal resolution of the sensor is determined by the time taken for the shutters to operate. Here, the shutter speed was set to 1μs. Further, the shortest time interval of continual ICCD operations is more than 2s, thus electron density measurement was carried out at a certain time in an arc discharge by controlling trigger-signal timings.

Electron densities in arc discharges are achieved by performing Abel transformation to line-integral electron densities. A line-integral electron density $\langle N_{ek}(x,y)\rangle L = \int_0^L N_e \mathrm{d}z$ is expressed by the following equation [9]:

$$\langle N_{ek}(x,y)\rangle L = -\frac{P}{f}\sum_{j=1}^{k}\frac{T_j(\lambda_1)-T_j(\lambda_2)}{\beta(\lambda_1^2-\lambda_2^2)} \quad (1)$$

where: x = Radial direction of arc discharge (m)
y = Axial direction of arc discharge (m)
z = Optical path direction (m)
L = Length of discharge area along z (m)
N_{ek} = Electron density at kth microlens (m^{-3})
P = Diameter of microlens (m)
f = Focal length of microlens (m)
$= 4.47\times10^{-16}$ (m)
λ = Wavelength of laser (m)

$T(\lambda)$ = Spot shift in x direction for wavelength λ (m)

A detailed description of analytical process has been previously reported [11].

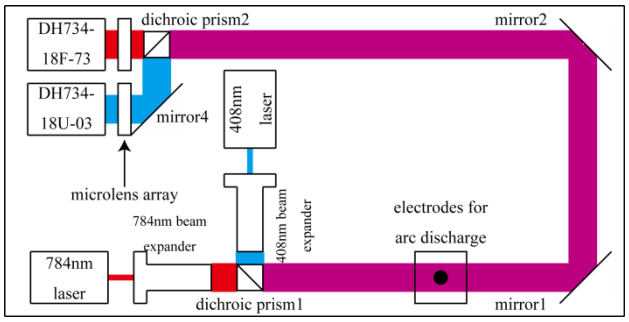

Fig. 1. A top view of the main components of the Shack-Hartmann type laser wavefront sensor

B. Circuit for arc discharge

The circuit for generating arc discharges is illustrated in Figure 2(a). A 2.5-μF capacitor was charged up to 8kV and through a current limiting resistance of 10 Ω, positive arc discharges were generated in 3-mm air gap between rod-to-rod tungsten electrodes of 1 mm in diameter. The peak value and damping time constant of an arc current was 0.8 kA and 25 μs as shown in Figure 2(b). The time when breakdowns occurred was defined as t=0s. The arc current at t=70 and 90μs was 50 and 20A, respectively. The applied voltages on the anode and arc currents were measured by a high voltage probe (NISSIN PULSE ELECTRONICS CO., LTD. EP50K) and a Rogowski coil (Power Electronic Measurements Ltd. CWT60LF R).

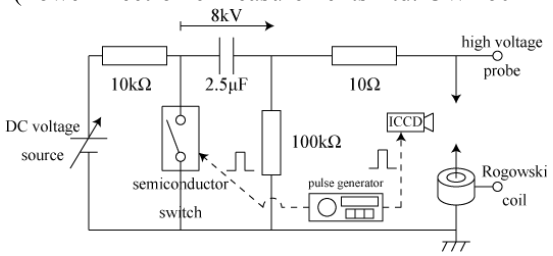

(a) The circuit for generating arc discharges

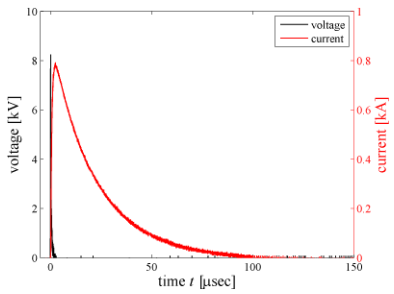

(b) Voltage and current waveforms

Fig. 2. Arc discharges

C. Emission light from arc discharge

Emission light from arc discharges was observed using a framing camera incorporating three ICCD cameras (Hamamatsu photonics K. K. C7977-01; minimum shutter speed=5ns). The shutter speed of each ICCD camera was set to 500ns.

III. Results

Figure 3(a) and (b) show typical spot shift vectors of 784- and 408-nm lights, respectively. The measurements were carried out at t=90μs. The spot shift vectors exemplified by the green solid lines were averaged along the y direction. Displacing the exemplified regions in the axial direction provided the moving average from the anode to cathode. The axial spatial resolution was 450μm due to the average among three spot shift vectors along the y direction. The radial spatial resolution, on the other hand, was 150μm, which is equal to the diameter of the microlenses.

Figure 4 shows the radial components of the averaged spot shift vectors indicated by the green solid lines in Figure 3. As shown in Figure 4, the presence of the electrons was confirmed by the difference between the spot shifts of the two lasers. Figure 5 represents the line-integral electron density given by using the spot shifts in Figure 4 and equation (1). The line-integral electron density was approximated by a Gauss function. Figure 6 shows the electron density acquired by performing Abel transformation to the Gauss function. In the same manner, overall electron density distributions in arc channels were achieved. Figure 7(a) and (b) show the overall electron density distributions at t=70 and 90μs, respectively. The red and blue regions indicate the highest and lowest electron densities in arc channels.

Figure 8(a) and (b) show emission light from arc discharges observed using the framing camera at t=70 and 90μs, respectively. The light intensity in Figure 8 increases from blue to red regions. The white regions represent the saturation of the light intensity.

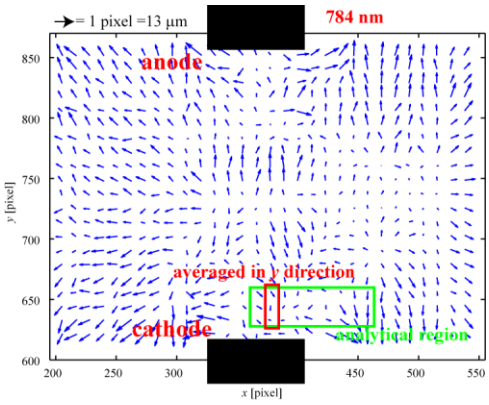

(a) 784-nm laser light

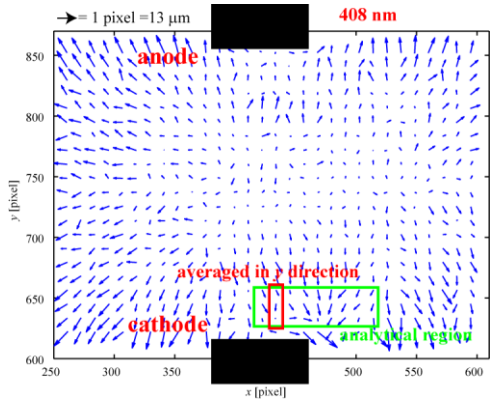

(b) 408-nm laser light

Fig. 3. Spot shift vectors

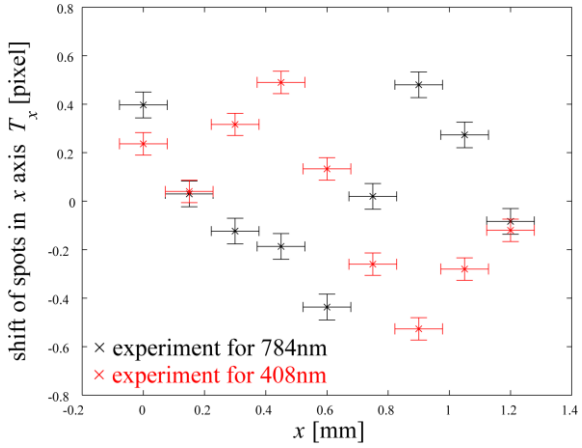

Fig. 4. The radial components of the averaged spot shift vectors

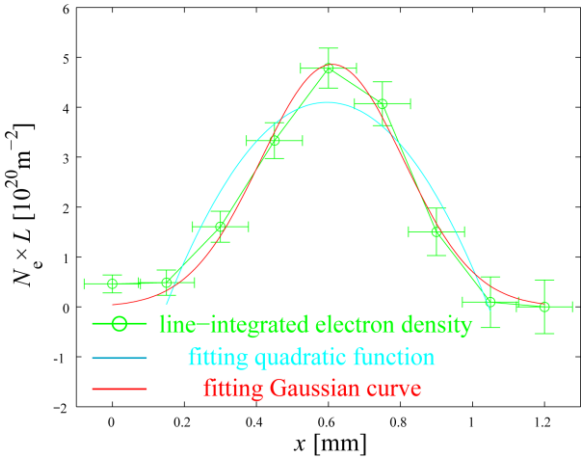

Fig. 5. The line-integral electron density

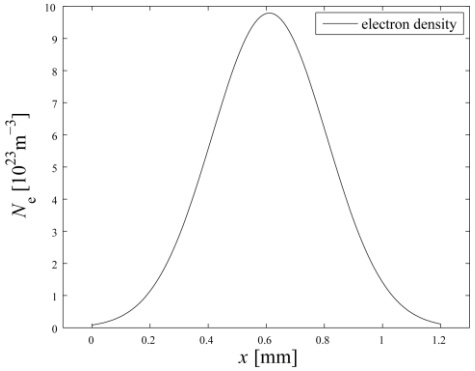

Fig. 6. The electron density

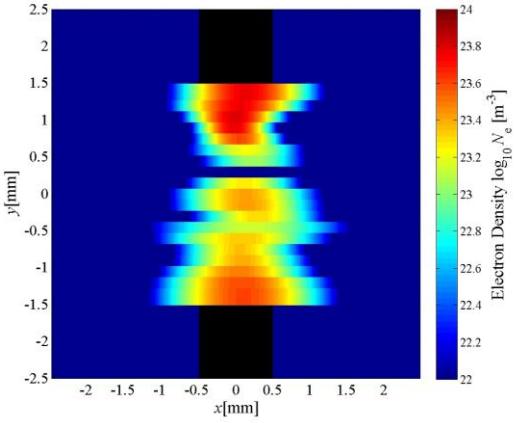

(a) t=70μs

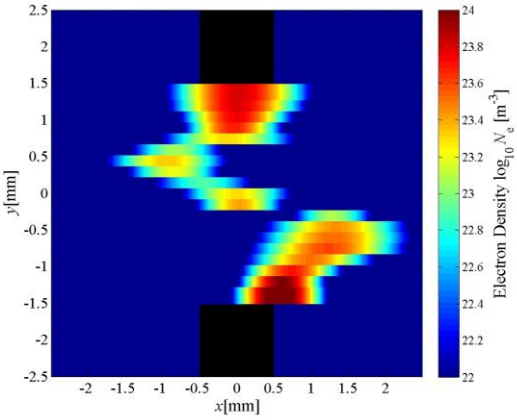

(b) t=90μs

Fig. 7. The overall electron density distributions

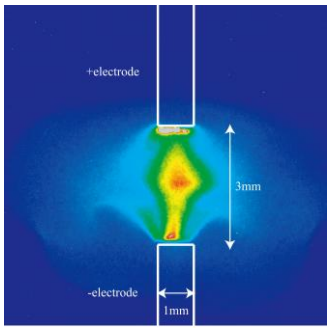

(a) t=70μs

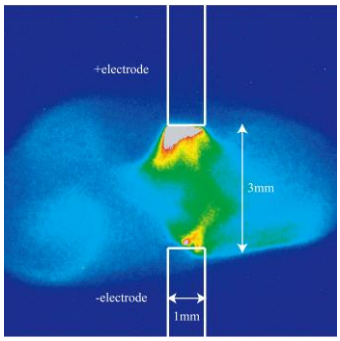

(b) t=90μs

Fig. 8. Emission light from arc discharges

IV. DISCUSSION

The electron densities in an extinguishing phase shown in Figure 7 were lower around the gap centre than near the anode and cathode. The same values of electron densities were not acquired among different arc discharges, but higher electron densities around both electrodes were reproducibly achieved. The behaviour of the electron densities around the anode is direct evidence supporting theoretical studies that have predicted an increase in electron densities with contaminating metallic vapour from an anode [13]. On the other hand, one of the most reasonable supports for higher electron densities around the cathode is the electron emission from the cathode due to the collision of positively charged ions.

The electron density distributions in Figure 7 are consistent with the images of emission light in Figure 8 because the regions representing stronger light intensity tend to have higher plasma densities including greater number densities of excited species and electrons.

V. CONCLUSION

We reported on an electron density distribution over an atmospheric arc channel obtained by a single measurement using a Shack-Hartmann type laser wavefront sensor. Electron densities in an extinguishing phase with currents of several tens of amperes were lower around the gap centre than near the anode and cathode. Shack-Hartmann sensor was demonstrated to be a valuable instrument for the quantitative observation of electron density distributions in unstable atmospheric arcs.

REFERENCES

[1] J.J. Gonzalez, R. Girard, A. Gleizes: "Decay and post-arc phases of a SF6 arc plasma: a thermal and chemical non-equilibrium model", *J. Phys. D; Appl. Phys.*, Vol. 33, No. 21, pp. 2759- 2768, 2000

[2] H. Cole, S. Epstein, J. Peace: "Particulate and Gaseous Emissions When Welding Aluminum Alloys", *JOEH*, Vol. 4, pp. 678- 687, 2007

[3] T. Inaba, T. Iwao: "Treatment of Waste by dc Arc Discharge Plasmas", *IEEE TDEI*, Vol. 7, No. 5, pp. 684- 692, 2000

[4] R. E. Orville, M. A. Uman, A. M. Sletten: "Temperature and Electron Density in Long Air Sparks", *J. Appl. Phys*., Vol. 38, , pp. 895- 896, 1967

[5] Masanori Akazaki, Katsunori Muraoka, Makoto Hamamoto: "Studies of an Atmospheric Impulse Arc Using a Two-Wavelength Laser Interferometry", *T.IEE Japan*, Vol. 101-A, No. 5, pp. 255- 262, 1981

[6] Kiichiro Uchino, Katsunori Muraoka, Masanori Akazaki: "Studies of an Atmospheric Impulse Arc by Ruby-Laser Scattering", *T.IEE Japan*, Vol. 103-A, No. 11, pp. 609-616, 1983

[7] J.B. Belhaouari, J.J. Gonzalez, A. Gleizes: "Simulation of a decaying SF6 arc plasma: hydrodynamic and kinetic coupling study", *J. Phys. D; Appl. Phys.*, Vol. 31, No. 10, pp. 1219- 1232, 1998

[8] A.B. Murphy, T. McAllister: "Modeling of the physics and chemistry of thermal plasma waste destruction", *Phys. Plasmas*, Vol. 8, pp. 2565- 2571, 2001

[9] Tetsuo Fukuchi, Yukihiro Yamaguchi, Takuya Nayuki, Koshichi Nemoto, Kiichiro Uchino: "Development of a laser wavefront sensor for measurement of discharge in air", *T.IEE Japan*, Vol. 122-A, No. 11, pp. 958- 964, 2002

[10] N. Qi, R. R. Prasad, K. Campbell, P. Coleman, M. Krishnan, B. V. Weber, S. J. Stephanakis, D. Mosher: "Laser wavefront analyzer for imploding plasma density and current profile measurements", *Rev. Sci. Instrum.*, Vol. 75, No. 10, pp. 3442- 3445, 2004

[11] Yuki Inada, Shigeyasu Matsuoka, Akiko Kumada, Hisatoshi Ikeda, Kunihiko Hidaka: "Development of Shack-Hartmann Type Laser Wavefront Sensor for Electron Density Measurement", Technical Meeting on Electrical Discharges, Static Apparatus and Switching and Protecting Engineering, *IEE Japan*, ED-10-034, SA-10-050, SP-10-001, 2010

[12] J. M. Geary: "Introduction to Wavefront Sensors", Tutorial Texts in Optical Engineering, Vol. TT18, SPIE, 1995

[13] J. M. Tehrani, E. Pfender: "Effects of Metallic Vapor on the Properties of an Argon Arc Plasma", *Plasma Chem. Plasma Process*, Vol. 4, No. 2, pp. 129- 139, 1984